UKRAINIAN JOURNAL OF MECHANICAL ENGINEERING AND MATERIALS SCIENCE

Vol. 5, No. 2, 2025

Iaroslav Lavrenko¹, Daniil Okladnikov²

Department of Dynamics and Strength of Machine and Strength of Materials, National Technical University of Ukraine "Igor Sikorsky Kyiv Polytechnic Institute", 37, Peremohy Avenue, Kyiv, Ukraine, E-mail: lavrenko.iaroslav@gmail.com.ua, ORCID 0000-0002-4384-4866
Faculty of Mathematics and Computer Science, Freiberg University of Mining and Technology, 6, Akademiestrasse, Freiberg, Germany,

E-mail: danok04012002@gmail.com, ORCID 0009-0000-6683-3871

INVESTIGATION OF THE STRESS–STRAIN STATE OF THE PLANET GEAR SHAFT AND CARRIER OF THE PLANETARY GEARBOX OF AN ELBOW ORTHOSIS

Received: August 22, 2025 / Revised: September 28, 2025 / Accepted: October 06, 2025

© Lavrenko I., Okladnikov D., 2025

https://doi.org/10.23939/ujmems2025.03.038

Abstract. Mechanical transmissions are widely used in various types of structures and mechanisms in different branches of the machine-building industry. One such branch is medicine. Devices with mechanical components are also used for patient rehabilitation in the postoperative period. Such mechanisms are known as orthoses. Structures of this type must meet several strict requirements—for example, compactness, light weight, safety, reliability, and others. Orthoses must reproduce the lost functions of a healthy person as accurately as possible. As previous work has shown, planetary gears meet the requirement for compactness. Planetary gears provide the necessary technical characteristics. This article presents the simulation and analysis of the stress-strain state of the components of a planetary gearbox for an elbow orthosis. KISSsoft and Ansys software packages were used for the design and 3D modeling of components, as well as for determining the stress-strain state. During the design process, KISSsoft software displays the profiles of the gear teeth and the contact line, allowing further adjustments to be made if necessary. When modeling the gears, the connecting elements were made of 45 steel. The article presents the basic formulas used for the analytical calculation and shows the stress and displacement fields obtained using the Ansys software product.

Keywords: Gearbox, stress, deformation, shaft, satellite, carrier shaft, Kisssoft, Ansys.

Introduction

In traumatology, selecting rehabilitation devices for patients undergoing treatment is a constant necessity. Such devices must meet several key requirements, including compact design, ease of use, reliability, and patient safety. Orthoses may differ in type and structural design. This work examines a mechanical orthosis, which plays a crucial role in postoperative rehabilitation.

Mechanical orthoses typically include an electric motor and a gearbox. The design of such devices requires careful determination of drive parameters and motor power to reproduce movements as closely as possible to those of a healthy elbow, particularly in terms of speed and force. The requirement for compactness can be fulfilled by using a planetary gearbox, which, due to multiple satellites, provides the necessary motion speed. The change in direction of the working elements can be achieved through a bevel gear transmission. Planetary gearboxes are distinguished by their small dimensions, stable operation, and high efficiency.

Problem Statement

Mechanical transmissions are often subjected to damage during operation under the influence of various factors. One of the primary causes of their failure is the occurrence of high stresses and deformations in the contact zones of moving elements and at the mounting points on shafts. Planetary

gearboxes, which are widely used in traumatology, consist of gear trains that operate at high rotational speeds. This creates the risk of overloads and consequently leads to the premature failure of the mechanism.

During the design process, it is essential to carefully consider the tooth geometry of the gears and the potential occurrence of contact stresses to ensure the reliability and durability of the gearbox. Since gears are mounted on shafts, modeling and analyzing the stress–strain state are critical stages in the development of mechanical orthoses.

Review of Modern Information Sources on the Subject of the Paper

In recent years, significant advances have been made in understanding the dynamic behavior of rotor systems. Numerous studies have focused on modeling both static and dynamic processes using various engineering software tools, such as Ansys, KISSsoft, Abaqus, and others. For instance, in [1], the dynamics of flexible rotors equipped with active magnetic bearings were analyzed using the finite element method (FEM) in Ansys Workbench. In [2], a detailed study of a stepped composite rotor shaft was conducted, including load analysis, boundary conditions, vibration characteristics, and the Campbell diagram.

Research in [3] investigated the stress-strain state (SSS) of a shaft using Ansys tools. In [4, 5], a model of an engine shaft was developed in CATIA, followed by static, dynamic, and fatigue analyses using Ansys. The study in [6] presents evaluations of strength and stiffness for shafts operating under high-torque conditions, which is particularly relevant for automotive and marine applications. The work in [7] focused on the early detection of structural weaknesses through the analysis of the static behavior of a pump shaft model under various loading scenarios using FEM.

In recent years, there has been a growing focus on optimizing shaft designs and evaluating their strength using the finite element method (FEM), particularly in applications where precision and reliability are crucial. In [8], approaches to shaft optimization considering their operational characteristics are described in detail. Reference [9] examines the application of the KISSsoft software for 3D modeling and stress analysis of shafts in planetary gearboxes used in mechanical elbow orthoses, including a comparative study based on von Mises and Tresca criteria. This highlights the importance of accurately designing drive components in orthoses, which must ensure safe and effective patient rehabilitation.

In [10], the influence of cracks on the dynamic characteristics and structural integrity of a rotating stepped shaft was investigated using FEM modeling. Analytical and numerical evaluations of the stress-strain state of hydraulic unit shafts, considering their specific structural features, are presented in [11]. Studies [12, 13] propose advanced modeling and optimization of the stress-strain state of high-strength rotor and shaft components used in high-speed machinery, including drive systems for orthoses.

In [14], a comprehensive study of the static and fatigue strength, as well as the bending stiffness, of a bevel-cylindrical gear shaft was conducted, which is essential for ensuring the reliable operation of gearboxes in orthoses. Finally, [15] analyzes the structural behavior and strength of a steel spool shaft used as a drive shaft in steel rope winding under progressively increasing loads—an example that can be applied in the development of orthosis drive mechanisms.

Thus, the study and optimization of shafts are key to creating high-performance orthoses that combine compactness, reliability, and durability, providing patients with a safe and effective rehabilitation process.

Objectives and Problems of Research

To develop a highly efficient and reliable design of a planetary gearbox that meets all technical requirements, a comprehensive design process and a detailed analysis of the stress-strain state of its components are necessary. Such an approach enables the identification of critical areas within the structure that may cause failures or malfunctions of the mechanism, which in turn can pose a potential safety risk to patients.

Iaroslav Lavrenko, Daniil Okladnikov

Numerical modeling of the stress-strain state plays a crucial role in the design phase, as it enables the prediction of the gearbox's behavior under operational loads. The application of the finite element method (FEA) significantly reduces calculation time compared to traditional methods described in technical literature, improves the accuracy of results, and minimizes the risk of errors. In this study, the KISSsoft and Ansys software packages were employed to perform calculations of the components of the planetary gearbox, providing a comprehensive and efficient approach to modeling and optimizing the design.

Main Material Presentation

According to the technical requirements and structural features of the intended mechanism, the output shaft of the planetary gearbox must be positioned perpendicular to the input shaft. This configuration can be achieved through a bevel gear transmission, as illustrated in Fig. 1 [8].

To achieve technical characteristics that closely replicate the motion of a healthy human joint, the overall gear ratio of the mechanism should be at least 110. This requirement ensures sufficient torque and precise movement control in the application. Since the maximum recommended gear ratio for a single planetary stage does not exceed 9, the gearbox must incorporate at least three planetary stages to meet this criterion.

From the standpoint of manufacturability, mechanical efficiency, and structural compactness, it is advantageous to design the gearbox using identical planetary stages [5]. This approach simplifies production, reduces costs, and ensures uniform performance across stages, which is particularly important in devices such as orthoses, where precision and reliability are crucial for safe and effective operation.

The mechanical orthosis proposed in the article consists of three identical planetary gear stages and one bevel stage, with an overall gear ratio of 125. Of particular interest for verifying the analytical calculations of stresses and deflections in shafts is the satellite shaft. This is due to the presence of a stress concentrator in the form of a flange and the absence of a fillet radius, which is present on other shafts, creating specific conditions for the distribution of stresses and deformations.

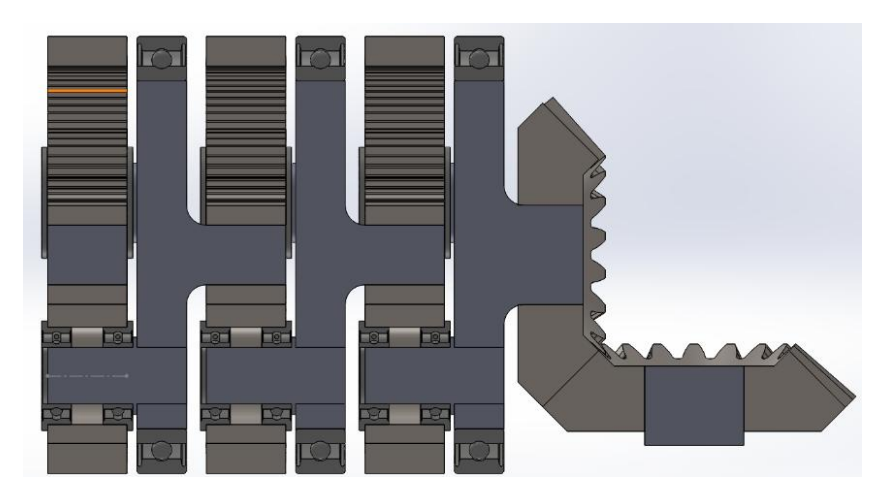


Fig. 1. 3D model of planetary gearbox for an elbow orthosis

The gears are selected sequentially in accordance with the design requirements. Their dimensions were determined using the KISSsoft software package in two stages. At the first stage, based on a minimal set of input data, such as gear module coefficients, wheel parameters, material properties, and applied loads, preliminary gear dimensions were estimated. At the second stage, these parameters were refined, taking into account specified ranges for the number of teeth, module, center distance, and other design requirements. Based on the finalized data, a detailed calculation is performed.

For modeling, gear material was chosen as grade 45 steel [8]. According to the technical specifications, the output shaft of the gearbox rotates at a speed of 2.8 s^{-1} , which means that the sun gear

of the final planetary stage rotates approximately five times faster. The power required for the mechanism's operation is 30 W.

Since it is necessary to study the stress–strain state of the satellite and carrier shafts, a boundary value problem in linear elasticity must be solved. Let us consider a body with volume Ω , bounded by surface S, made of an isotropic material, with small deformations.

Assume that at the initial moment. t_0 The actual body has zero displacements $U_i(\vec{x},t_0)$, strains $\varepsilon_{ij}(\vec{x},t_0)$, and stresses $\sigma_{mn}(\vec{x},t_0)$. Subsequently, over a specific period of time, the load conditions within the volume Ω and on parts of its surface change $S_G = S_U \cup S_P$. At time t, the following are applied: surface forces. $\overline{P}_m(\vec{x},t)$ on the portion of the surface S_P ; prescribed displacements $\overline{U}_i(\vec{x},t)$ on the portion of the surface S_U .

Then, to determine at each point of the body the following quantities: displacements $U_i(\vec{x},t)$; strains $\varepsilon_{ii}(\vec{x},t)$; stresses $\sigma_{mn}(\vec{x},t)$.

The equilibrium equation is a special case of the equation of motion (1)

$$\nabla_n \sigma_{mn} = 0. \tag{1}$$

Geometric relations (for small deformations) (2)

$$\varepsilon_{ij} = \frac{1}{2} \left(\nabla_i U_j + \nabla_j U_i \right), \tag{2}$$

And only elastic deformations are considered (3)

$$\varepsilon_{ii} = \varepsilon_{ii}^{e} \,, \tag{3}$$

physical equations (4)

$$\varepsilon_{ij}^{e} = C_{ijmn} \sigma_{mn} \,, \tag{4}$$

where C_{iimn} – compliance tensor.

Additionally, boundary conditions are applied on $S_U(5)$ and $S_P(6)$:

$$U_i|_{S_{ij}} = \overline{U}_i, \tag{5}$$

$$\sigma_{mn} v_n \Big|_{S_p} = \overline{P}_m \,. \tag{6}$$

For convenience in solving the boundary value problem, the principle of virtual displacements is commonly applied.

To derive the equation of the principle of virtual displacements, the above relations are used along with the symmetry properties of the stress tensor. $\sigma_{mn} = \sigma_{nm}$ and the Gauss–Ostrogradsky theorem. As a result, the following functional is obtained with respect to variations of displacements and the corresponding strains (7):

$$F = \int_{\Omega} \sigma_{mn} \delta \varepsilon_{mn} d\Omega - \int_{S_P} \overline{P}_m \delta U_m dS = 0, \qquad (7)$$

together with the kinematic boundary conditions on the surface S_U , defines an infinite set of possible (virtual) stress-strain states.

For the application of the finite element method, it is necessary to transition to matrix notation [11]. Hooke's law can be expressed as (8)

$$\{\sigma\} = [D]\{\varepsilon^e\},\tag{8}$$

where [D] – stiffness matrix.

In the case of elastic isotropy of the material, the matrix takes the form (9):

$$[D] = 2G \cdot \begin{pmatrix} a & b & b & 0 & 0 & 0 \\ b & a & b & 0 & 0 & 0 \\ b & b & a & 0 & 0 & 0 \\ 0 & 0 & 0 & c & 0 & 0 \\ 0 & 0 & 0 & 0 & c & 0 \\ 0 & 0 & 0 & 0 & 0 & c \end{pmatrix}, \tag{9}$$

where $2G = E/(1+\mu)$; $a = (1-\mu)/(1-2\mu)$; $b = \mu/(1-2\mu)$; c = 0.5; E - Young's modulus; μ - Poisson's ratio.

All deformations are elastic (10):

$$\{\varepsilon\} = \{\varepsilon^e\} \ . \tag{10}$$

Taking into account (10), expression (8) can be written as (11):

$$\{\sigma\} = [D]\{\varepsilon\} \ . \tag{11}$$

The geometric equations take the form (12):

$$\{\varepsilon\} = [B]\{q\}_{e}, \tag{12}$$

where $\{q\}_e = \{(q^1, q^2, q^3)_1, ..., (q^1, q^2, q^3)_M\}^T = \{q_1, q_2, ..., q_{3M}\}^T$ – finite element nodal displacement vector; [B] – the differentiation matrix with respect to global coordinates, associated only with the type of finite element and the global coordinate system.

The functional, taking into account the possibility of superposition of work in finite elements – because finite elements interact with each other at the nodes and do not overlap – is expressed as follows (13):

$$F = \sum_{e} \int_{\Omega^{e}} \{\delta q\}_{e}^{T} [B]^{T} [D] [B] \{q\}_{e} d\Omega - \sum_{e} \int_{S_{p}^{e}} \{\delta q\}_{e}^{T} [\phi]^{T} \{p\} dS = 0,$$
(13)

where the load vectors are denoted $\{p\} = \{\overline{p}_1, \overline{p}_2, \overline{p}_3\}^T$; S_P^e – the side of the finite element that lies on the surface S_P of the body.

Since the integrands contain vectors $\{\delta q\}_{\rm e}^{\rm T}$ and $\{q\}_{\rm e}$, which do not depend on the integration parameters and can therefore be taken outside the integrals. By grouping the integrals, we obtain (14):

$$F = \sum_{e} \{ \delta q \}_{e}^{T} \int_{\Omega^{e}} [B]^{T} [D] [B] d\Omega \cdot \{ q \}_{e} + \sum_{e} \{ \delta q \}_{e}^{T} \int_{S^{e}} [\phi]^{T} \{ p \} dS = 0.$$
(14)

Let us denote (15):

$$[K]_e = \int_{\Omega^e} [B]^T [D] [B] d\Omega, \qquad (15)$$

and (16)

$$\{P\}_{e} = \int_{S_{e}^{e}} [\phi]^{T} \{p\} dS.$$
 (16)

Then

$$F = \sum_{e} \{\delta q\}_{e}^{T} ([K]_{e} \{q\}_{e} - \{P\}_{e}) = 0.$$
(17)

Since the displacement variations are arbitrary, the system of linear algebraic equations takes the form (18):

$$[K]{q} = {P},$$
 (18)

with respect to the global vector of actual displacement increments $\{q\}_{\rm e}$ at the nodes of the finite element mesh.

Mechanical properties of the material and dimensions of the satellite shaft are given in Table 1 [9].

	Table 1
Material properties and dimensions of the satellite sha	ft

Parameter	Units of measure	Steel 45
Density	kg/m ³	7850
Thermal expansion coefficient	C ⁻¹	1.2·10 ⁻⁵
Young modulus	Pa	2.1011
Poisson's ratio		0,3
Shear modulus	Pa	$7.69 \cdot 10^{10}$
Shaft diameter	mm	6
Shaft length	mm	10.4
Collar diameter	mm	7

According to the characteristics given in Table 1, the KISSsoft program was used to model the satellite shaft and the planetary transmission. The modeling results are shown in Fig. 2.

In the process of designing the shafts of a planetary gearbox, a critical task is to ensure a reliable connection between the planet gears and the carrier, allowing the planet gears to rotate freely around their own axes. To achieve this, the planet gears are mounted on separate shafts fixed within the airline, while the gear is installed on bearings. A schematic and a 3D model of such a shaft are shown in Fig. 2. To provide stable and durable gear mounting, thrust bearings are employed. To prevent axial displacement of the bearings, a collar with a height of 1 mm and a length of 0.4 mm is formed on the shaft.

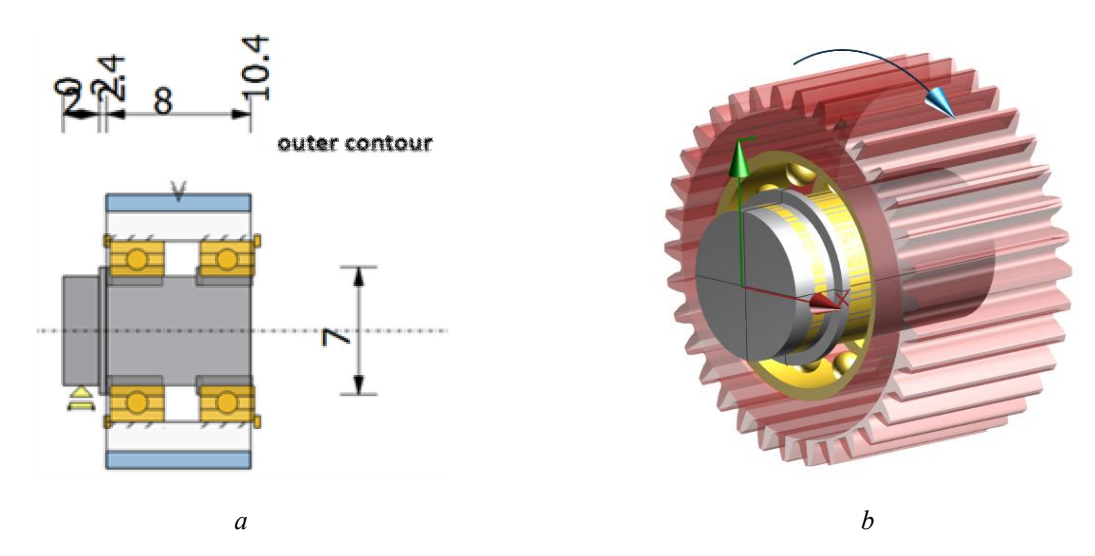


Fig. 2. Satellite and satellite shaft: a – Satellite shaft drawing; b – Satellite model

The only loads on the shaft are two bearings, i.e., two forces perpendicular to the shaft axis. To determine their magnitudes, a load is applied to planet gear 3 of the planetary stage, as it experiences the most significant load. According to the technical specifications, the maximum torque acting on the output shaft is 1.732 N·m. Figure 3 shows the forces acting on the carrier.

Where M is the torque on the bevel gear, and P is the force acting on the side of the satellite shaft, directed perpendicular to the radius drawn to the point of application from the carrier center. The equation for the moment equilibrium is equal to zero with respect to the center of the carrier (19):

$$M - 3Pa_w = 0, \quad P = \frac{M}{3a_w},$$
 (19)

Iaroslav Lavrenko, Daniil Okladnikov

where a_w the center distance of the sun-planet gear transmission. Substituting the numerical values, we obtain $P = 47.26 \ N$. An equal-magnitude force acts on the satellite shaft. The masses of the shaft, gear, and bearings are not taken into account.

The planet gear is rigidly fixed in the carrier. Fig. 4 shows the calculation scheme for modeling in Ansys.

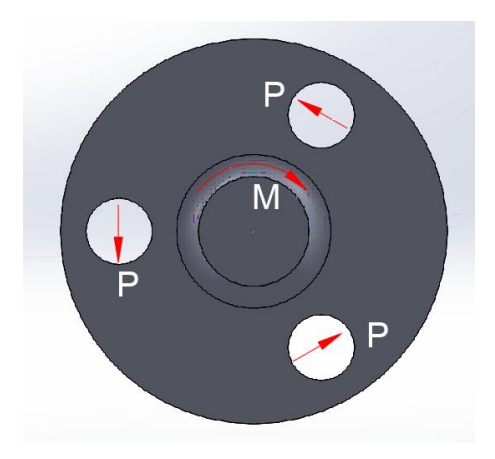


Fig. 3. Forces acting on the carrier

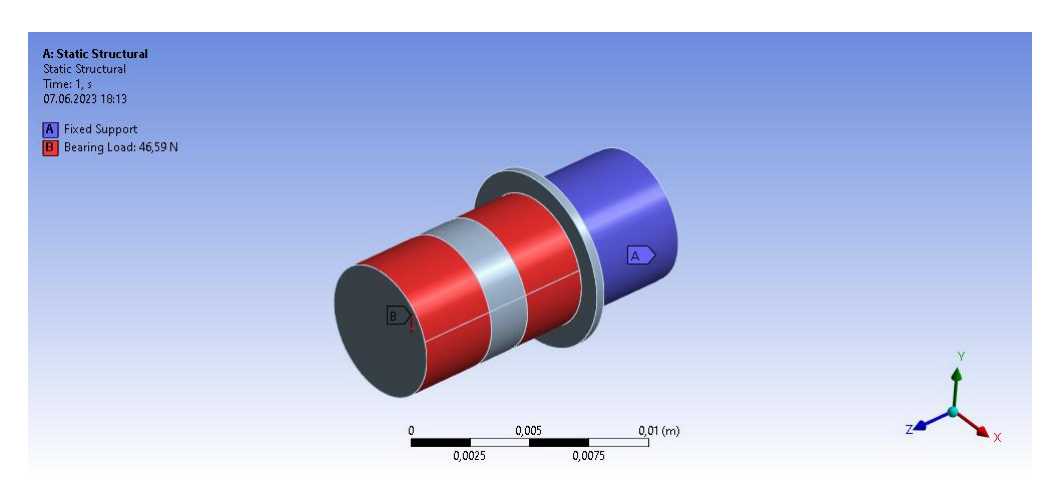


Fig. 4. Calculation scheme for modeling: A – fixed support, B – P force

Fig. 5 shows the stress state of the shaft (equivalent von Mises stress), and Fig. 6 shows the deformed state of the shaft (deflection).

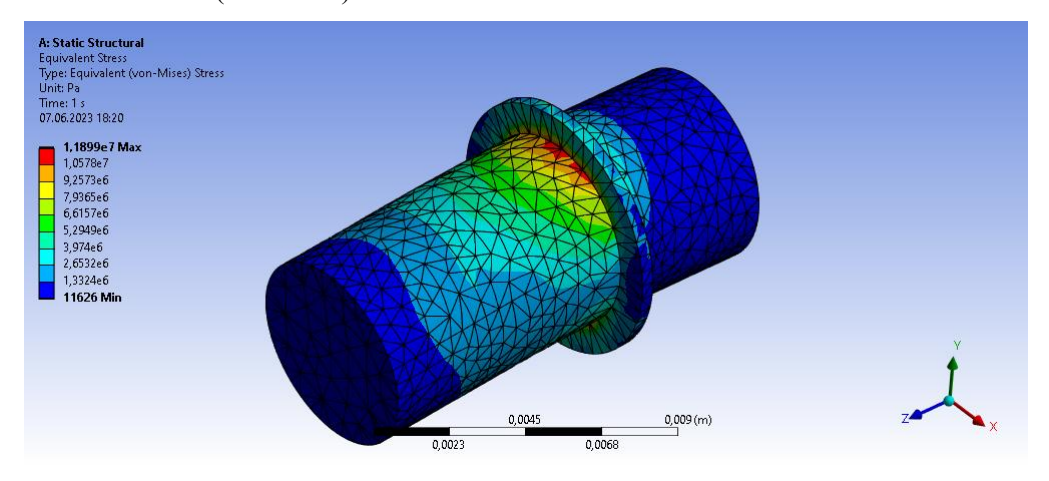


Fig. 5. Stress distribution (von Mises), Pa

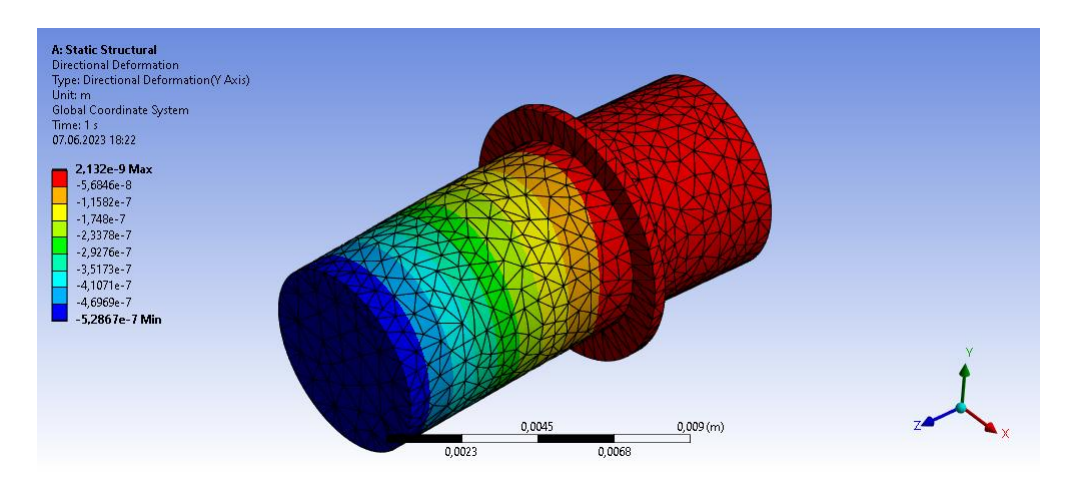


Fig. 6. Shaft deflection, m

The results obtained by numerical and analytical methods (stress concentration was not considered) are presented in Table 2.

Comparative analysis of the calculation

Table 2

	Numerically	Analytically
Stress at the collar–shaft junction, MPa	12.90	9.54
Maximum deflection, mm	5.29·10 ⁻⁴	5.4·10 ⁻⁴
Maximum stress, MPa	12.90	10.74

From Table 2, it can be seen that the discrepancy in stress at the collar–shaft junction is approximately 35 %, indicating a stress concentration factor of 1.35. Meanwhile, the values of the maximum deflections are almost identical, with a deviation of only 2 %.

We also consider the stress-strain state of the carrier of the 3rd stage, which simultaneously serves as the shaft of the bevel gear. Its schematic is shown in Fig. 7, and Table 3 presents the mechanical properties of the material and the dimensions of the shaft.

Table 3
Material properties and dimensions of the carrier shaft

Parameter	Units of measure	Steel 45
Density	kg/m ³	7850
Thermal expansion coefficient	C ⁻¹	1.2·10 ⁻⁵
Young modulus	Pa	$2 \cdot 10^{11}$
Poisson's ratio		0,3
Shear modulus	Pa	$7.69 \cdot 10^{10}$
Shaft diameter	mm	30
Shaft length	mm	14
Collar diameter	mm	10

Fig. 8 shows the calculation scheme for modeling in Ansys.

Fig. 9 shows the stress state of the shaft (equivalent von Mises stress), and Fig. 10 shows the deformed state of the shaft (deflection).

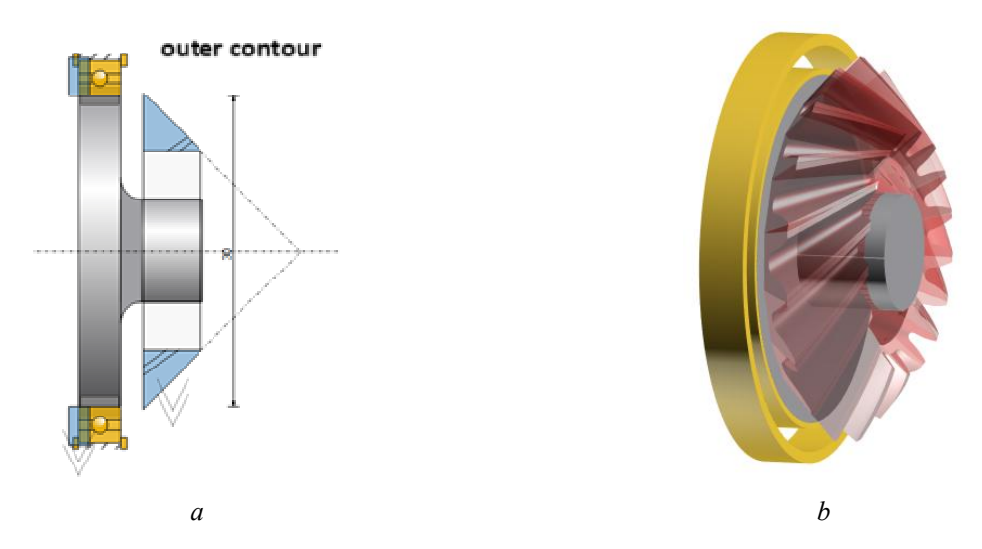


Fig. 7. Carrier and carrier shaft: a – Carrier shaft drawing; b – Carrier model with bevel gear

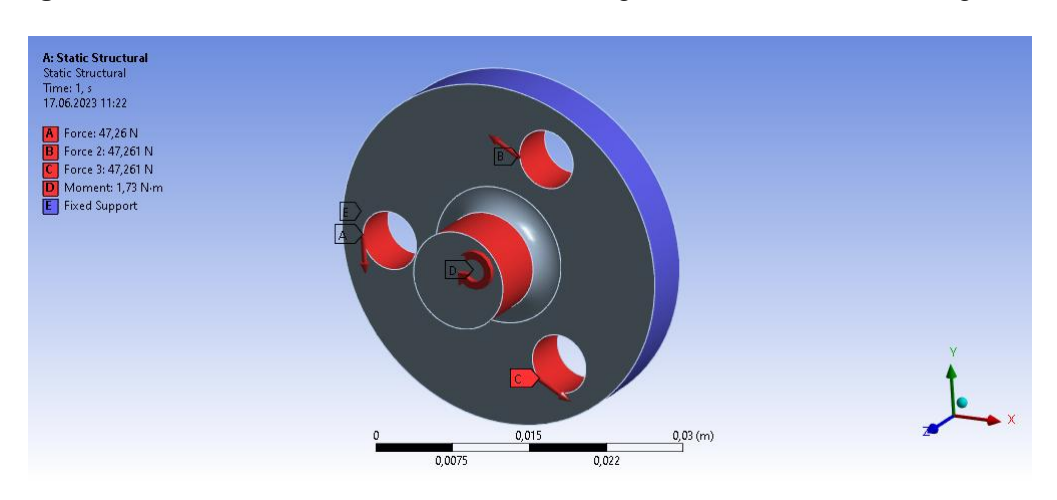


Fig. 8. Calculation scheme for modeling: E – fixed support, A,B,C – P force; D – M moment

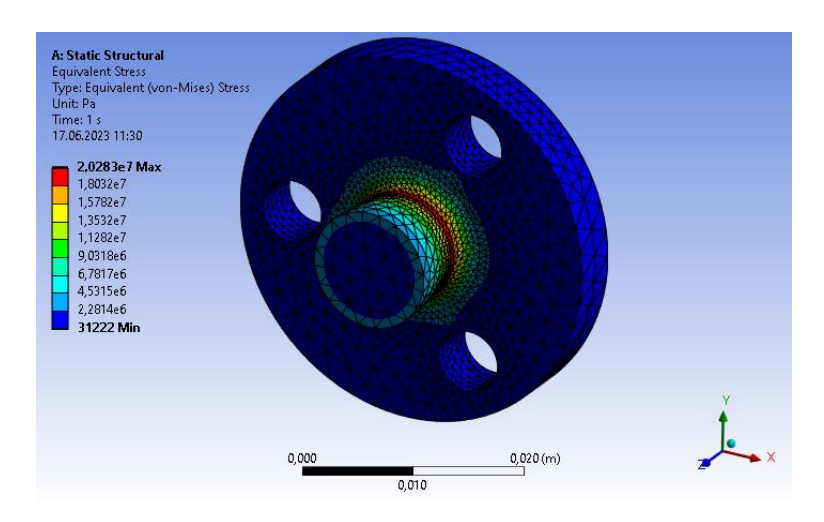


Fig. 9. Carrier stress distribution (von Mises), Pa

The results obtained by numerical and analytical methods (stress concentration was not considered) are presented in Table 4.

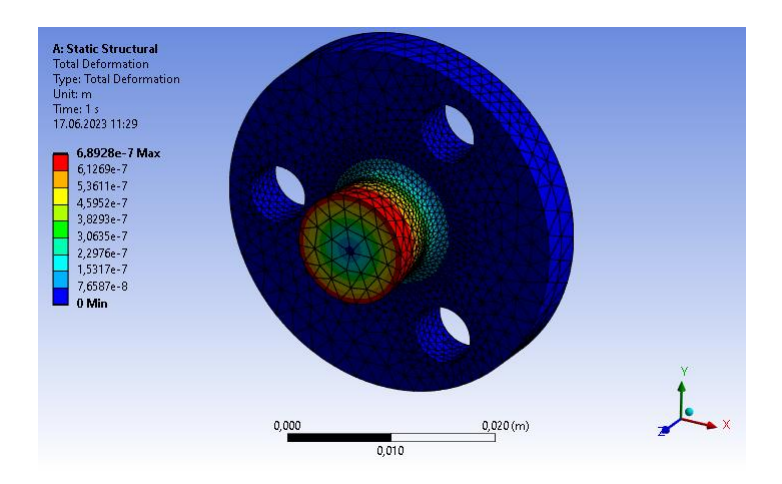


Fig. 10. Carrier deflection, m

Comparative analysis of the calculation

NumericallyAnalyticallyMaximum stress, MPa20.2824.43Maximum deflection, mm0.000680.00071

Table 4

From Table 4, it can be seen that the discrepancy in stress at the collar–shaft junction is approximately 20 %, which can be attributed to the fact that the analytical calculation did not account for the presence of a fillet radius, where the highest stresses occur. At the same time, the values of the maximum deflections are almost identical, with a deviation of only 2 %.

Conclusions

In this paper, we designed a gearbox for an elbow orthosis. The design was carried out using the KISSsoft software package, which utilizes the ISO 6336 standard for calculating gear strength.

Although the collar diameter of the satellite shaft is only 1 mm, the stress concentration is significant, with a stress concentration factor of 1.35. Nevertheless, the maximum stress of 12.9 MPa is considerably lower than the material's yield strength of 240 MPa. Therefore, the strength requirement for the satellite shaft is satisfied.

The numerical calculation of the carrier, on the other hand, showed an overestimation of the acting stresses by approximately 20 %. However, this does not affect the fulfillment of the strength and stiffness requirements, indicating that the carrier has been correctly designed.

References

- [1] S. M. Ghoneam, et al., "Dynamic analysis of rotor system with active magnetic bearings using finite element method", *International Journal of Engineering Applied Sciences and Technology*, Vol. 7, Issue 1, ISSN No. 2455-2143, pp. 09–16, 2022.
- [2] Iaroslav Lavrenko, Maksym Sushchenko, Oleksii Ishchenko, "Frequency response and strength analysis of the elbow orthosis planetary gearbox shaft using FEA", *Ukrainian Journal of Mechanical Engineering and Materials Science*, Vol. 9, No. 4, 2023, pp. 27–41.
- [3] N. Lenin Rakesh, et al., "Stress analysis of a shaft using Ansys", *Middle-east Journal of Scientific Research*, 12 (12), ISSN 1990-9233, pp. 1726–1728, 2012.
- [4] B. Gaikwad Rushikesh, and V. Gaur Abhay, "Static and dynamic analysis of shaft (EN24) of foot mounting motor using FEA", *International Journal of Innovations in Engineering Research and Technology*, Vol. 5, Issue 6, ISSN: 2394-3696, pp. 57–70, 2018.

Iaroslav Lavrenko, Daniil Okladnikov

- [5] Iaroslav Lavrenko, Maksym Sushchenko, Olena Chaikovska, "Simulation of the Gears stress-strain state of Elbow Orthosis Planetary Gearbox", *Ukrainian Journal of Mechanical Engineering and Materials Science*, Vol. 10, No. 2, 2024, pp. 33–45.
- [6] P. Krishna Teja, et al., "Finite element analysis of propeller shaft for automotive and naval application", *International Research Journal of automotive Technology*, Vol. 1, Issue 1, ISSN 2581-5865, pp. 8–12, 2018.
- [7] A. Asonja, et al., "Analysis of the static behavior of the shaft based on finite method under effect of different variants of load", *Applied Engineering Letters*, Vol. 1, No. 1, pp. 8–15, ISSN 2466-4847, 2016.
- [8] Iaroslav Lavrenko, Daniil Okladnikov, "Design and strength analysis of the planetary gearbox shafts for an elbow orthosis using Kisssoft", *Ukrainian Journal of Mechanical Engineering and Materials Science*, Vol. 11, No. 1, 2024, pp. 37–43.
- [9] J. Joshi, et al., "Design analysis of shafts using simulation softwares", *International Journal of Scientific and Engineering Research*, Vol. 5, Issue 8, ISSN 2229-5518, pp. 751–761, 2014.
- [10] M. J. Jweeg, et al., "Dynamic analysis of a rotating stepped shaft with and without defects", *IOP Conf. Series: Materials Science and Engineering, 3rd International Conference on Engineering Sciences*, Kerbala, Iraq, 2020, Vol. 671.
- [11] S. Culafic, and D. Bajic, "Analytical and numerical analysis of shafts' stress and strain states of the hydropower unit", *International Scientific Journal "Machines. Technologies. Materials"*, Vol. XV, Issue 8, pp. 294–298, 2021.
- [12] C. Gong, et al., "High-strength rotor design for ultra-high speed switched reluctance machines", in *IEEE Transactions on Industry Applications*, 2020, Vol. 56, Issue: 2, pp. 1432 1442.
- [13] M. E. Gerlach, et al., "Mechanical stress and deformation in the rotors of a high-speed PMSM and IM", *Elektrotechnik und Informationstechnik*, Vol. 138, Issue 2, pp. 96–109, 2021.
- [14] N. F. Timerbaev, et al., "Software systems applications for shaft strength analysis in mechanical engineering", *Procedia Engineering*, Vol. 206, pp. 1376–1381, 2017.
- [15] N. Rasovic, et al., "Design and analysis of steel reel shaft by using FEA", *Tehnicki vjesnik*, Vol. 26, Issue 2, pp. 527–532, 2019.